Structural and Thermodynamic Study on Short Metal Alkanoates: Lithium Propanoate and Pentanoate

F. J. Martínez Casado,[†] M. Ramos Riesco,[‡] M. V. García Pérez,[‡] M. I. Redondo,[‡] S. López-Andrés,[§] and J. A. Rodríguez Cheda*[,‡]

E.S.R.F. (BM16), 38043 Grenoble, France, Departamento de Química Física I, Facultad de Ciencias Químicas, Universidad Complutense, 28040 Madrid, Spain, and Departamento de Crystalografía y Mineralogía, Facultad de Ciencias Geológicas, Universidad Complutense, 28040 Madrid, Spain

Received: May 21, 2009; Revised Manuscript Received: July 29, 2009

Lithium propanoate and pentanoate were characterized by DSC, single crystal and powder XRD and FTIR and impedance spectroscopies. Lithium propanoate presents a solid-to-solid transition (SII−SI) at $T_{ss} = (549.1 \pm 0.7)$ K on first heating that varies on the second and next ones, followed by a fusion at $T_f = (606.1 \pm 0.5)$ K. For lithium pentanoate, two solid-to-solid transitions (SIII−SII and SII−SI), at $T_{ss} = (205.5 \pm 0.5)$ K and $T_{ss} = (325.2 \pm 0.7)$ K, respectively, and a melting point at $T_f = (576.5 \pm 0.3)$ K were found. The crystal structures for both compounds were characterized at 100 and 298 K (and for the lithium propanoate also at 160 K). Single-crystal XRD showed that the SII phase of both compounds has a monoclinic structure with the same symmetry group ($P2_1/c$). This is the first time that a single-crystal structure has been reported for any member of the lithium alkanoates series, so far. FTIR and impedance spectroscopies were also carried out to better characterize the solid phases in these compounds.

1. Introduction

One of the most interesting aspects of the organic salts in general, and metal alkanoates in particular, is the *polymorphism* and/or *polymesomorphism* that they present. Thereby, different solid (plastic crystal, *rotator*, or *condis*) or fluid *mesophases* (*liquid crystal*), as well as polymorphs in the crystal phase, can be found in these salts. The study of the structure and behavior of the different phases in these families of organic salts is of great interest in the field of the *step-wise melting* process, involving all of the transitions (solid-to-solid or/and melting) taking place from a totally ordered crystalline phase at low temperature to the isotropic liquid. This process can be rather complicated, as in thallium(I) alkanoates[1,2] or lead(II) alkanoates.[3]

Nowadays, the study of lithium compounds has become fundamental because of their use in lithium-ion batteries.[4,5] These kinds of batteries are the most widely used portable energy source due to their high-energy density, compact design, and long lasting life. Lithium ions are hosts in both the positive and the negative electrodes. Specifically, mixed oxides and phosphates with lithium and transition metals are being developed as cathodes in these systems.[6] In this sense, also of great interest would be the use of mixed organic salts of lithium with another metal as those found for some binary systems (e.g., lithium cesium butanoate [LiC4 + CsC4][7] or lithium rubidium butanoate [LiC4 + RbC4][8]) as *precursors* of those oxides.

Lithium alkanoates (LiC*n*, where *n* is the total number of carbons in the alkanoate anion, hereafter) have been studied for the last 50 years[9] by several techniques, such as adiabatic calorimetry,[10−12] DSC,[13−18] XRD,[17,19−21] dilatometry,[22] and others. However, many aspects about the thermal behavior of the series and about the structure of the interesting phases they present are still not explained.

Although the number of studies developed in the lithium alkanoates series is very high, only the crystal structure of some hydrated lithium alkanoates (e.g., lithium formate monohydrated[23] or the lithium acetate dihydrated[24,25]) has been determined. Some of the structures of longer members (LiC8 to LiC19)[17] were studied by powder XRD at room temperature. A triclinic structure is reported from these data, which is very dissimilar to the one found in this work. In both compounds, LiC3 and LiC5, two of the cell axes and the beta angle vary slightly (the third axis being dependent on the length of the alkyl chain), in a monoclinic cell. Therefore, and in our knowledge, this is the first time that the structure of two members of the lithium alkanoates series have been characterized by single-crystal XRD.

In this paper, the nature of the transitions and the solid phases of lithium propanoate (LiC3) and pentanoate (LiC5) is discussed. Special attention will be paid to the strange thermal behavior shown by the LiC3 and on what seems to be an intermediate rotator phase by LiC5, similar to the one found for the lead(II) alkanoates[3,26] or in the alkyl ammonium salts.[27,28]

2. Experimental Section

2.1. Sample Preparation. Lithium propanoate (LiC3) was synthesized and purified following two methods. The first one, (i) consisting of the chemical reaction between Li_2CO_3 (Aldrich, 99.9%) and propionic acid (Fluka, ≥ 99.5 %) in deionized water, has been described elsewhere.[10,13] The product was later purified by dissolution in methanol and fractional precipitation with ethyl ether (Aldrich, 99+%). The second method used (ii) consists of the reaction between lithium hydroxide ($LiOH \cdot H_2O$, Fluka, ≥99%) and propionic acid (Fluka, ≥ 99.5 %) in acetonitrile (Aldrich, 99.5+%). The lithium propanoate was recrystallized in 1-propanol/2-propanol (Fluka, ≥ 99.5 %; Panreac, 99%, respectively) several times and vacuum dried. Special attention

* Corresponding author. Tel.: +91-3944306. Fax: +91-3944135. E-mail: cheda@quim.ucm.es.
[†] E.S.R.F. (BM16).
[‡] Facultad de Ciencias Químicas, Universidad Complutense.
[§] Facultad de Ciencias Geológicas, Universidad Complutense.

10.1021/jp9047715 CCC: $40.75
Published on Web 09/08/2009

TABLE 1: Experimental Parameters and Main Crystallographic Data for the Studied Compounds

data	LiC3a		LiC3b	LiC5	
empirical formula	$LiC_3H_5O_2$		$LiC_3H_5O_2$	$LiC_5H_9O_2$	
M_r ($g \cdot mol^{-1}$)	80.01		80.01	108.06	
crystal system	Monoclinic		Monoclinic	Monoclinic	
space group (No.)	$P2_1/c$ (14)		$P2_1/c$ (14)	$P2_1/c$ (14)	
crystal size (mm)	0.10 × 0.08 × 0.01		0.02 × 0.01 ×0.003	0.08 × 0.06 × 0.007	
temperature (K)	100(2)	298(2)	160(2)	100(2)	298(2)
a (Å)	9.6090(19)	9.823(2)	9.6460(19)	14.181(3)	14.358(3)
b (Å)	4.9410(10)	4.9330(10)	4.9320(10)	4.8890(10)	4.9410(10)
c (Å)	8.6480(17)	8.8120(18)	8.6980(17)	8.6300(17)	8.8460(18)
β (°)	94.99(3)	96.86(3)	95.36(3)	95.81(3)	93.92(3)
V (Å^3)	409.03(14)	423.94(15)	411.99(14)	595.3(2)	626.1(2)
Z	4	4	4	4	4
λ (Å)	0.7514	0.7514	0.9786	0.7514	0.7514
D_c ($g \cdot cm^{-3}$)	1.299	1.254	1.290	1.206	1.146
μ (mm^{-1})	0.10	0.10	0.10	0.09	0.08
reflection collected	831	888	330	1230	1246
reflections with $I > 2\sigma(I)$	810	833	323	812	844
parameters refined	100	60	55	109	73
hydrogen treatment	all H-atom parameters refined	H-atom parameters not refined (geom.)	H-atom parameters not refined (geom.)	only H-atom coordinates refined	H-atom parameters not refined (geom.)
R-factor	0.035	0.048	0.034	0.082	0.070
wR-factor	0.096	0.134	0.086	0.218	0.216
goodness of fit	1.042	1.222	1.266	1.061	0.954
CCDC deposition numbers	731735	731736	731737	731738	731739

was paid to the purity of the sample to avoid the formation of acid soap[29−35] or the presence of water.

LiC5 was obtained by the reaction between lithium hydroxide ($LiOH \cdot H_2O$, Fluka, ≥99%) and valeric acid (Fluka, ≥ 99 %), using ethanol (Merck, >99.8%) as solvent. The salt was purified dissolving it in methanol (Merck, ≥99.8%), filtered, and then precipitated with 2-propanol (Panreac, 99%), repeating the process at least twice. This method is slightly different from others described in the literature.[10,14]

Even when lithium formate and lithium acetate are hygroscopic and their hydrates known, in our experience, lithium propanoate and lithium pentanoate are not. We used though dry solvents for preparation or crystallization of both, but it was not really necessary. Through the FTIR and DSC techniques, we followed systematically a water control on the samples, and we never found a hydrate of any of them. At the same time, we were always aware of handling the samples trying to avoid long periods in contact with the atmosphere.

DSC purity determinations, averages of at least three measurements, were 99.97% and 99.82% for LiC3 (synthesized following the above described methods (i) and (ii), respectively) and 99.98% for LiC5.

Lithium alkanoates grow into flake-shaped crystals. Thus, crystallization in both compounds (LiC3 and LiC5) produced very tiny crystals, and the sizes are given in Table 1. Crystals suitable for X-ray studies were grown by slow evaporation from solutions of compounds in methanol/ether (1:1) and methanol/2-propanol (1:1) for LiC3 and LiC5, respectively.

2.2. Differential Scanning Calorimetry. A TA Instruments DSC, model Q10, was used to register all the thermograms. Tightly sealed aluminum volatile pans were utilized, in dry nitrogen, flowing at 50.0 $mL \cdot min^{-1}$. A MT5 Mettler microbalance was used to weigh the samples, ranging between 3 and 10 mg (with an error of ±0.001 mg). The calorimeter was calibrated in temperature using standard samples of In and Sn, supplied by TA (purity >99.999% and >99.9%, respectively), and of benzoic acid (purity >99.97%), supplied by the former NBS (lot 39i), and in enthalpy with the In and Sn standards already described.

All the measurements were done at a heating rate of 5 $K \cdot min^{-1}$. All the scans were usually explored from 200 K to the temperature corresponding to the isotropic liquid in each case (a maximum of 650 K).

2.3. Single-Crystal Diffraction. Two different crystals were used in the case of LiC3 (LiC3a and LiC3b), and only one was used for LiC5. X-ray measurements were conducted using synchrotron radiation (with $\lambda = 0.7514$ Å for LiC3a and LiC5, and $\lambda = 0.9786$ Å for LiC3b) at the BM16 Spanish beamline of ESRF with a CCD detector (ADSCq210rCCD), making phi scans when collecting the data. Each compound was measured at different temperatures: 100, 160, and 298 K for LiC3 (the crystal LiC3a being used for the first and last temperatures and LiC3b for the intermediate one) and 100 and 298 K for LiC5. After several measurements, the crystals suffer some radiation damage.

The structures were solved by direct methods and subsequent Fourier synthesis using the SHELXS-97 program[36] and were refined by the full-matrix least-squares technique against F^2 in anisotropic approximation for all non-hydrogen atoms with the SHELXL-97 program.[37] The treatment of the hydrogen atoms was different depending on the quality of the crystals: for LiC3a (at 100 K), all the parameters for the hydrogen atoms were refined; for LiC5 (at 100 K), only the positions were refined, with isotropic atomic displacements (Uiso); in the case of LiC3a (at 298 K), LiC3b, and LiC5 (at 298 K), the hydrogens were calculated geometrically.

The main crystallographic data and some experimental details are shown in Table 1.

As can be inferred from the solved crystals, the structure in these compounds is bilayered (ionic and lipidic layers). The joint between these latter layers is very weak, and it is of great difficulty to obtain good crystals due to their ease to exfoliate.

Further crystallographic details for the structures reported in this paper may be obtained from the Cambridge Crystallographic Data Center (see Supporting Information).

2.4. X-ray Powder Diffraction. XRD measurements were carried out with a Philips X'Pert PRO MPD X-ray diffractometer with vertical goniometer θ/θ (Cu $K_{\alpha 1}$ radiation, 1.54056 Å, Ni filter) and X'Celerator detector, equipped with a high-temperature chamber Anton Paar HTK1200. The in situ XRD area was scanned from $2\theta = 2°-70°$ at several temperatures in the

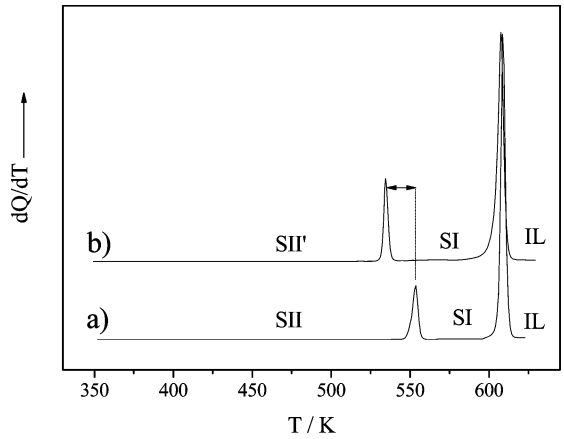

Figure 1. DSC thermogram of LiC3, in the first (a) and second and following (b) heatings.

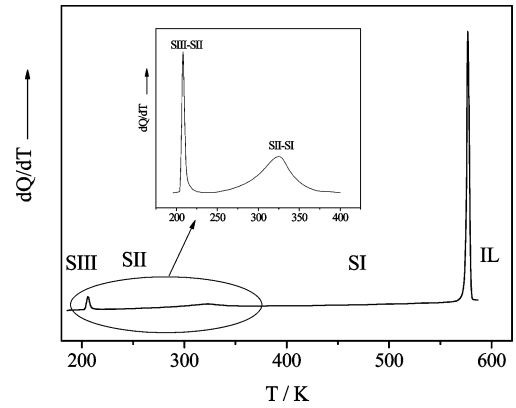

Figure 2. Details of DSC thermogram of LiC5, showing the SIII−SII and SII−SI transitions.

range from room temperature to 600 K during the heating and the cooling, at a rate of 3 K·min^{-1}.

2.5. FTIR Spectroscopy. Mid-infrared spectra of the samples in KBr pellets and powders between two pure KBr pellets were recorded at a resolution of 4 cm^{-1} in a Nicolet Magna 750 FTIR spectrometer. No significant differences between the spectra obtained by both procedures were observed. A commercial variable-temperature cell, SPECAC VTL-2, adapted for solid samples was employed to obtain IR spectra at different temperatures.

2.6. Impedance Spectroscopy. Sintered cylindrical pellets of known surface and thickness, pasted with silver electrodes on both faces, were used for electrical measurements. Impedance spectroscopy measurements were conducted in function of temperature and frequency, using HP4284A and HP4285A precision LCR meters to obtain the electrical conductivity. Measurements were carried out under a N_2 flow to ensure an inert atmosphere.

3. Results

3.1. Thermal Analysis. The thermal behavior of the two compounds was analyzed by DSC. Two phase transitions are found for the LiC3: a solid-to-solid transition (SII−SI) and a fusion (SI−IL), at 549.1 K (in the first heating) and 604.1 K, respectively. The temperature of the solid-to-solid transition varies between 5 and 25 K in the second and following heatings (see Figure 1), if there is no waiting time, and recovers the initial temperature with time. For instance, a LiC3 sample stored for two years in our lab showed the same initial thermogram. This odd behavior will be discussed in section 4.

In the case of the LiC5, two solid-to-solid transitions (SIII−SII and SII−SI) and a fusion are observed at 205.5, 325.2, and 576.5 K, respectively (Figure 2). Apart from the analysis of the solid phases, which will be discussed later, two special features are noticeable for the two solid-to-solid transitions: (a) due to its high undercooling effect, the SIII−SII transition is only detected if the sample is cooled at least until 173 K and maintained at this temperature for 5 min and (b) the SII−SI transition occurs in a very broad range of temperatures (250−370 K), as a noncooperative phenomenon. A detailed thermogram showing both solid-to-solid transitions is shown in Figure 2.

The thermal data values (Table 2) agree with those found in the literature for LiC3[13] and LiC5,[10,14] except the enthalpy of the SII−SI transition of the LiC5 with a slightly lower value than the one given by Franzosini et al.[10] In that case, the measurement was carried out by adiabatic calorimetry (calculating directly the value of the heat capacity), which is much more reliable for these kinds of broad transitions.

3.2. X-ray Diffraction. Both single-crystal and powder x-ray diffractions were used to study LiC3 and LiC5. The structures for both compounds were obtained by single-crystal XRD, at two different temperatures. In the case of LiC3, the SII phase is the stable crystalline phase from low temperature up to 549 K and was measured at 100, 160, and 298 K. Its structure at 100 K is represented in Figure 3. Two of the three crystalline phases (SIII and SII at low and room temperature) were characterized for the LiC5, at 100 and 298 K, respectively. No structural differences were found between them, and only a decrease in the density for the SII phase was observed, as can be inferred from the crystal data. The crystal arrangement for the low-temperature phase (SIII) is shown in Figure 4. Crystal data for the four measured crystals are given in Table 1.

The same symmetry, $P2_1/c$, is found for all the crystals, showing a bilayered arrangement, which is typical for most of the metal alkanoates.[3,38−41] There are ionic layers (lithium cations and carboxylate anions) alternating with lipidic layers (alkyl chains).

The structure for both compounds is fixed by the ionic layer, as can be inferred from the similar values of the b, c, and β parameters for LiC3 and LiC5. This result disagrees with the structures proposed by White et al.[17] for compounds from LiC8 to LiC19 at room temperature, where all the parameters (in a triclinic structure) seem to vary strongly between each other.

Even the tilt angle (regarding the layers) of the alkyl chains is similar: about 30 and 31° for LiC3 and LiC5, respectively, very close to the calculated value for the sodium and potassium alkanoates (30 and 33°, respectively).[42,43] Thus, it seems to be correct to extrapolate that the structure for other lithium n-alkanoates will be the same, fixed by the ionic order, as proposed by Ferloni et al.[9]

The only significant difference between the members of the lithium alkanoates series comes from the anion length, which marks the d-spacing values. These values were measured from powder x-ray diffraction data and are plotted as a function of the temperature in Figure 5. In this sense, the increase of the d-spacing from SII to SI in the LiC3 is remarkable, and it will be discussed later.

The tetrahedral coordination for the lithium ion found in these compounds is very stable from the electrostatic point of view.[44] Thus, a steady 2-D structure is formed in the ionic layer (see Figures 3B and 4B), strong enough to explain the high melting point observed for the lithium alkanoates,[9] despite the weak

TABLE 2: Temperatures, Enthalpies, and Entropies of the Transitions of the Pure Compounds

compound		transition	T/K	ΔH/kJ·mol^{-1}	ΔS/J·mol^{-1}·K^{-1}
LiC3	(i)	SII−SI[a]	549.1 ± 0.7	3.2 ± 0.1	5.7 ± 0.2
		SI−IL	606.1 ± 0.5	16.4 ± 0.2	27.1 ± 0.4
	(ii)	SII−SI[a]	549.7 ± 0.7	3.1 ± 0.1	5.6 ± 0.2
		SI−IL	606.4 ± 0.5	16.3 ± 0.2	26.9 ± 0.4
LiC5		SIII−SII	205.5 ± 0.5	1.31 ± 0.05	6.3 ± 0.3
		SII−SI	325.2 ± 0.7	3.0 ± 0.1	9.3 ± 0.3
		SI−IL	576.5 ± 0.3	21.74 ± 0.03	37.71 ± 0.07

[a] Referred to the S−S transition in the 1st heating of the LiC3.

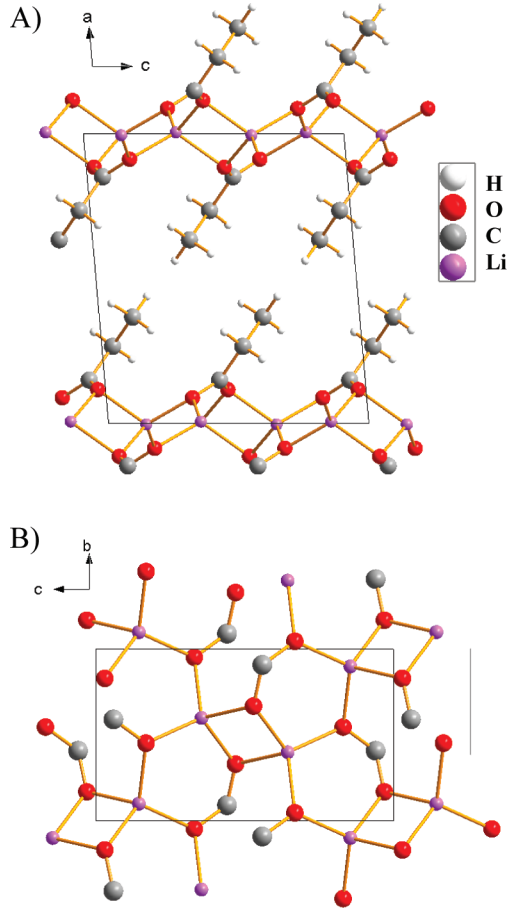

Figure 3. Crystal structure for the LiC3 at 100 K (LiC3a): (A) *ac* projection and (B) *cb* projection (H atoms and non-carboxylic C atoms not shown).

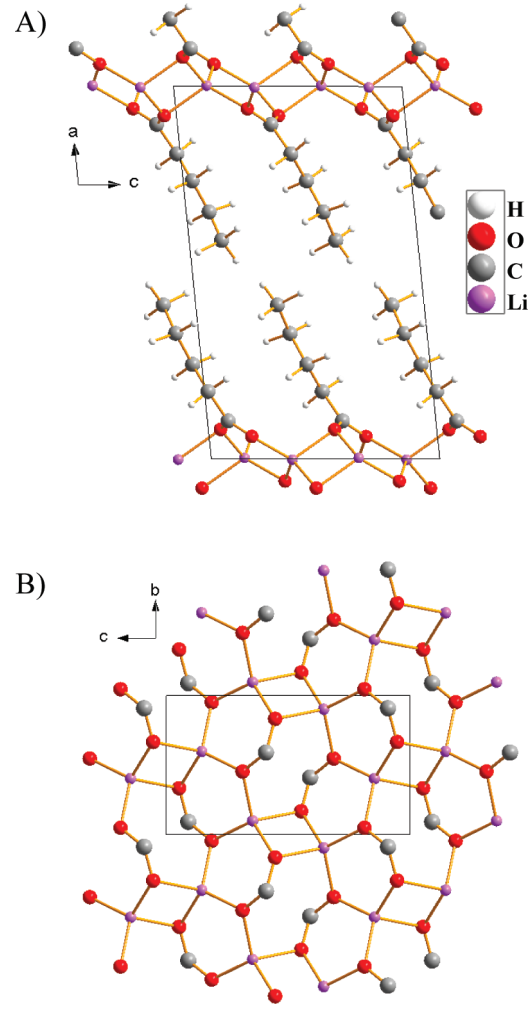

Figure 4. Crystal structure for the LiC5 at 100 K (LiC5a: (A) *ac* projection and (B) *cb* projection (H atoms and non-carboxylic C atoms not shown).

interaction between lipidic layers. Actually, both compounds could be considered as 2-D lithium coordination polymers (see Figures 3B and 4B). This aspect adds a special interest to these compounds in the porous material research area.[45]

3.3. FTIR. Room-temperature FTIR spectra of LiC3 and LiC5 (SII phases in both cases) are shown in Figure 6. Bands corresponding to aliphatic CH_2 and CH_3 stretching vibrations are observed below 3000 cm^{-1}. Methyl and methylene bending vibrations are also measured between 500 and 1400 cm^{-1}. In the LiC5 spectrum, three wagging progression bands are detected in the region 1100−1350 cm^{-1} corresponding to the all-trans alkyl chain present at this temperature. The short alkyl chain length in LiC3 doesn't allow the existence of such progressions. Both spectra show two symmetric ν_s (1447 and 1412 cm^{-1} in LiC5 and 1466 and 1442 cm^{-1} in LiC3) and asymmetric ν_{as} (1578 and 1559 cm^{-1} in LiC5 and 1584 and 1561 cm^{-1} in LiC3) carboxylate stretching bands. The wavenumber difference between asymmetric and symmetric COO^- stretching ($\Delta = \nu_{as} - \nu_s$), Δ = 120−130 cm^{-1}, is in agreement with the carboxylic bridging coordination observed by XRD. On the other hand, the presence of two bands for the carboxylate stretching vibrations is also in relation with the two CO distances (1.254 and 1.277 Å) measured in the XRD data file of the single-crystal structures for the studied compounds. No bands corresponding to the acid in any of the samples are observed which shows the high purity of both samples.

4. Discussion

a. LiC3. The anomalous shift in (SII−SI) transition temperature described in section 3.1 was already reported by other authors[10,13,46] but without any convincing explanation. It was first attributed to a "metastable fusion"[13] or to a "sluggish transition" ("some sluggishness still exhibited by solid-state

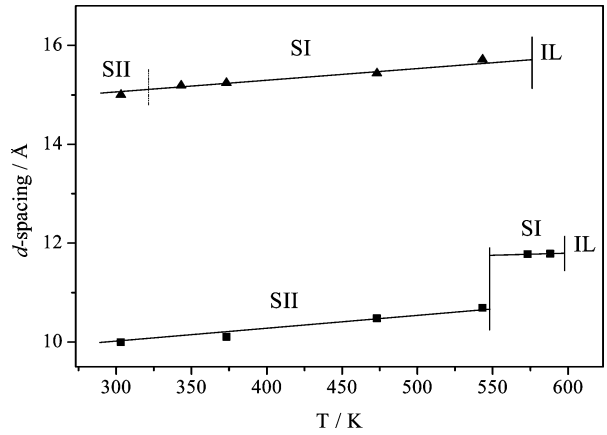

Figure 5. *d*-Spacing at high temperatures for the LiC3 (■) and the LiC5 (▲), indicating the phases and the transitions.

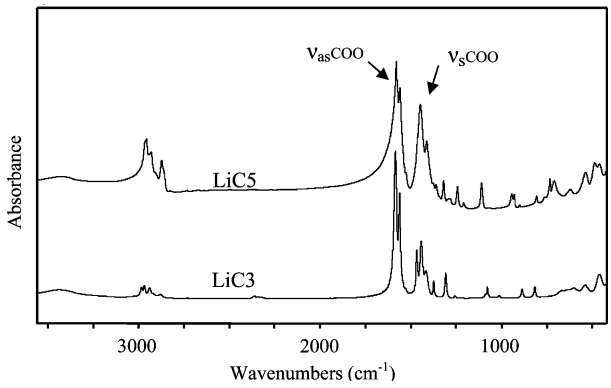

Figure 6. Room-temperature FTIR spectra of LiC3 and LiC5 (SII phases).

transition of the propanoate", *sic*.)[10] or just being ignored[46] when solving the binary phase diagram between lithium and cesium propanoates.

In this work, special attention has been paid to explain this strange transition. LiC3, with such a small alkyl chain, can not present a conformational disorder transition because there are not enough C atoms to form *gauche* defects in the chain. Thus, we considered first the possibility of having a propionic acid impurity with a possible formation of an acid soap.[29,31] This was ruled out because of the care taken during the synthesis avoiding the excess of acid and because of the absence of an additional big congruent or incongruent melting of this possible acid soap. On the other hand, an identical thermal behavior was found for the two different samples obtained by different methods of synthesis (section 2.1): the enthalpy and temperature of fusion were the same for all the samples within the experimental error, and both showed this transition moving. Moreover, the DSC purity determinations in the melting peak of the different samples gave always a high purity value. Systematic FTIR studies on the samples did not show any band corresponding either to the OH or to the CO of the acid groups. Besides, no acid was detected either by acid−base titration with Na_2CO_3 in water (this is the method used to eliminate any contamination of acid from the metal acid soaps).[31] Finally, the initial thermal behavior (first heating) was recovered in the LiC3 after 2 years, indicating the stability of the sample and showing that the thermodynamic behavior corresponds to the first heating, with a higher temperature for this transition.[47] Therefore, the nature of this solid-to-solid transition has to be related to a metastable phase, associated to a kinetic phenomenon and not to an impurity in the sample.

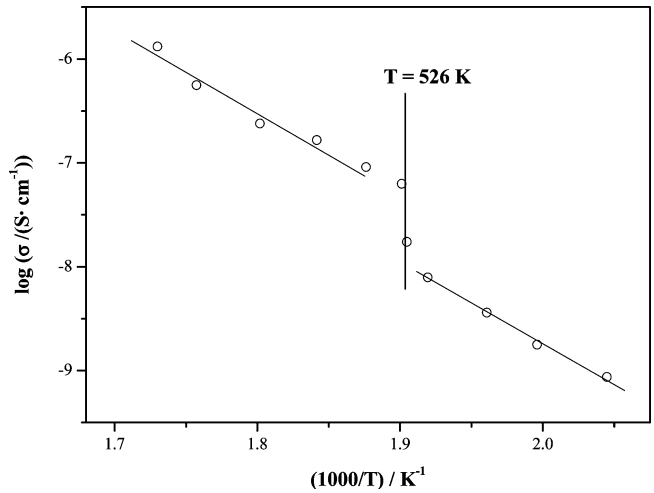

Figure 7. Arrhenius plot for the conductivity of LiC3 in the SII−SI transition.

Electrical conductivity measurements were decisive to characterize this solid-to-solid transition. Conductivity of the sample vs temperature was recorded, as described in the Experimental Section. The Arrhenius plot (Figure 7) shows a discontinuity in conductivity at 526 K, corresponding precisely to the SII−SI transition in the second and following heatings. The activation energies above and under the transition present values of 152 ± 10 and 149 ± 7 kJ·mol^{-1}, respectively. Theses energies were analyzed previously by Cingolani et al.,[48] and although a discrepancy is found for the value at lower temperatures, the one above the transition agrees perfectly.

Thus, this transition could be explained in principle as a melting of a crystalline subnet or a *premelting* phenomenon: an increase of the mobility of the ions in the solid state previous to the melting point.[49−51] This premelting effect has been largely studied for other compounds, e.g., silver salts[52] or Na and Li metasilicates.[49] Although the conductivity values of LiC3 are not as high as those of silver salts (in the superionic state), the effect is comparable.[49]

In short, the most probable explanation would be that SII−SI transition for the LiC3 involves the mobility of the Li^+ ions inside the subnet formed by the propanoate anions. This would be supported by the results obtained by powder X-ray diffraction (Figure 3), where an increase of the spacing between layers was observed in the transition.

b. LiC5. Two solid-to-solid transition and the fusion are found for the LiC5, as has been described in section 3.1.

Regarding the first transition (SIII−SII), the two solid-phase structures were determined by single-crystal diffraction. Apparently, there is no structural difference between them, and no disorder was found in the alkyl chain. Only a very slightly larger separation between methyl groups is detected for the SII phase. On the other hand, although the enthalpy for this transition is comparable to the one for methyl group rotation in similar compounds like *n*-butane (2.8 kJ·mol^{-1})[53] or 1,3,5-trichloro-2,4,6-trimethylbenzene (2.4 kJ·mol^{-1}),[54] this rotation always takes place at very low temperatures of 15−40 K, as it happens with the latter compound and the lithium acetate dihydrated.[55]

Therefore, if the methyl rotation is ruled out, the most plausible explanation for the origin of this transition would be an isostructural solid−solid transition involving solely a change in density: high density in solid (SIII) and low density in solid (SII). Both solids have the same symmetry and differ only in

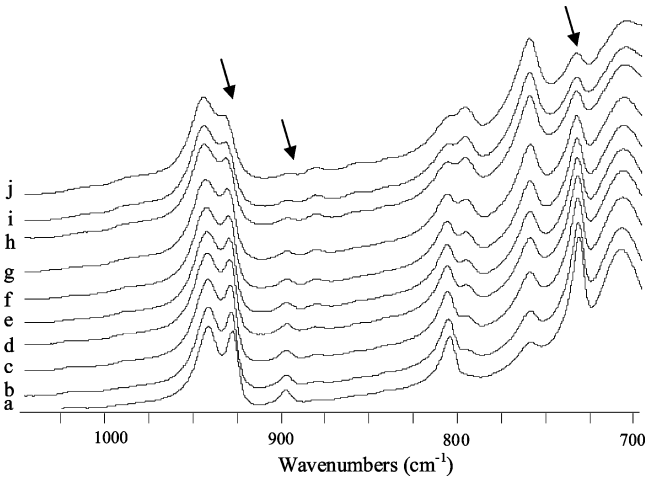

Figure 8. FTIR spectra of the LiC5 as a function of the temperature, where a, 296; b, 306; c, 316; d, 321; e, 326; f, 331; g, 338; h, 353; i, 363; j, 373 K.

their density,[56−59] as is found for the 1,2,4,5-tetrabromobenzene[60] or the *m*-carboxyphenylammonium monohydrogen phosphite,[61] both with a transition between two phases with a $P2_1/c$ structure.

The second solid-to-solid transition (SII−SI) appears for the LiC5 as a very broad band, as described in section 3.1. FTIR measurements were carried out to understand its nature.

Gradual changes are noticeable in the FTIR spectra as a function of the temperature (Figure 8), between 700 and 1000 cm^{-1}, from 296 up to 353 K (a and h, in Figure 8, respectively), without any change above this temperature (i and j), which corresponds approximately to the end of the broad transition. Specifically, there are three important bands, marked in the figure, at a frequency of 720, 890, and 920 cm^{-1}. On one hand, an intensity decrease can be seen in the band at 720 cm^{-1}, corresponding to the in-phase rocking vibration of the CH_2 groups in an all-trans conformation of the alkyl chain. The same evolution is detected in the other two bands, at 890 and 920 cm^{-1}, which correspond to terminal C−C stretching vibrations and CH_3 wagging vibrations, respectively. These features may indicate that the SII−SI transition could involve some kind of noncooperative conformational disorder (or a lambda transition) in the alkyl chain: from an all-trans conformation to a phase where the chains of the pentanoate anion present some *gauche* defects, as happens in the *condis* phases of the thallium(I) alkanoates.

However, to distinguish between the *condis* and *rotator* phase[26] it is very important to pay attention to the value of the cross-section area of the alkyl chains (S'), that is, the space that the alkyl chain has to form *gauche* defects. The area per polar head (S) calculated from the crystal structure of LiC5 in SII has a value of 21.8 $Å^2$. Taking into account the tilt angle of the chains with respect to the ionic layer (31°), S' can be calculated as $S' = S \cdot \cos 31°$. This yields a result of 18.7 $Å^2$ for the SII phase at 298 K, where the SII−SI transition has already started. Thus, although this calculated value for S' belongs to the SII phase, as it is a noncooperative transition (without having an abrupt change in the structure, as can be inferred from Figure 3), this value can be extrapolated for the SI phase. Accordingly, S' is comparable to the values obtained for the *rotator* phases of *n*-alkanes (20 $Å^2$),[62] lithium *n*-hexadecanoate (20.7 $Å^2$),[63] or Langmuir monolayers of alkyl chain surfactants in water (19.7−20.2 $Å^2$).[64,65] It is important to note that *rotator* phases allow certain conformational defects in the alkyl chains,[66] such as *kink* or *end-gauche* defects.

5. Conclusions

A thorough study (powder and single-crystal XRD and DSC) of lithium propanoate and lithium pentanoate was carried out, this being the first time that single-crystal structural data for any member of the lithium alkanoates series have been reported, so far.

The work was complemented with FTIR and impedance spectroscopies to characterize some of the solid phases found for these compounds. In this sense, important features have been detected for LiC3 and LiC5, emphasizing the *premelting* effect found for the LiC3 and the possible formation of an intermediate *rotator* phase in the LiC5. Although more studies are needed to clarify these points, this rotator phase (present also in other organic salts, as lead(II) alkanoates[3,26] or alkyl ammonium salts[27,28]) could also be the nature of the already studied intermediate phase for longer members of this lithium series.[9,17]

Acknowledgment. Partial support of this research by the Beca de Especialización en Organismos Internacionales (ES-2006-0024) and by the DGICYT of the Spanish Ministerio de Ciencia e Innovación (Project CTQ2008-06328/BQU) is gratefully acknowledged. The authors wish to thank the CAI's (Centro de Asistencia a la Investigación) of XRD and Spectroscopy of the UCM and BM16 (ESRF) for the use of their technical facilities. Special thanks too to Prof. J. Santamaría and J. García Barriocanal (Dpto de Física Aplicada III, Facultad de Ciencias Físicas, Universidad Complutense, Madrid, Spain) for the electrical conductivity measurements.

Supporting Information Available: The structures reported in this paper may be obtained from the Cambridge Crystallographic Data Center, on quoting the depository numbers CCDC-731735 and CCDC-731736, for LiC3a (at 100 and 298 K, respectively), CCDC-731737, for LiC3b (160 K), and CCDC-731738 and CCDC-731739, for LiC5 (at 100 and 298 K, respectively). This material is available free of charge via the Internet at http://pubs.acs.org.

References and Notes

(1) Cheda, J. A. R.; Redondo, M. I.; García, M. V.; Lópezde la Fuente, F. L.; Fernández Martín, F.; Westrum, E. F. *J. Chem Phys.* **1999**, *111* (8), 3590–3598.
(2) García, M. V.; Redondo, M. I.; Lópezde la Fuente, F. L.; Cheda, J. A. R.; Westrum, E. F.; Fernández Martín, F. *Appl. Spectrosc.* **1994**, *48* (3), 338–344.
(3) Martínez Casado, F. J.; García Pérez, M. V.; Redondo Yélamos, M. I.; Cheda, J. A. R.; Sánchez Arenas, A.; López de Andrés, S.; García-Barriocanal, J.; Rivera, A.; León, C.; Santamaría, J. *J. Phys.Chem. C* **2007**, *111* (18), 6826–6831.
(4) Guyomard, D.; Tarascon, J. M. *Adv. Mater.* **1994**, *6* (5), 408–412.
(5) Megahed, S. *J. Power Sources* **1994**, *51* (1−2), 79–104.
(6) Whittingham, M. S. *Chem. Rev.* **2004**, *104*, 4271–4301.
(7) Mirnaya, T. A.; Yaremchuk, G. G.; Prisyazhnyi, V. D. *Liq. Cryst.* **1990**, *8*, 701–705.
(8) Martínez Casado, F. J.; Ramos Riesco, M.; Cheda, J. A. R. *J. Therm. Anal. Calorim.* **2007**, *87* (1), 73–77.
(9) Ferloni, P.; Westrum, E. F. *Pure Appl. Chem.* **1992**, *64* (1), 73–78.
(10) Franzosini, P.; Westrum, E. F. *J. Chem. Thermodyn.* **1984**, *16*, 81–90.
(11) Franzosini, P.; Ngeyi, S. P.; Westrum, E. F. *J. Chem. Thermodyn.* **1986**, *18*, 609–618.
(12) Franzosini, P.; Ngeyi, S. P.; Westrum, E. F. *J. Chem. Thermodyn.* **1986**, *18* (12), 1169–1181.
(13) Ferloni, P.; Sanesi, M.; Franzosini, P. *Z. Naturforsch* **1975**, *30a* (11), 1447–1457.
(14) Ferloni, P.; Zangen, M.; Franzosini, P. *Z. Naturforsch* **1977**, *32a* (6), 627–631.
(15) Sanesi, M.; Ferloni, P.; Franzosini, P. *Z. Naturforsch* **1977**, *32a* (10), 1173–1177.
(16) Franzosini, P.; Sanesi, M.; Cingolani, A.; Ferloni, P. *Z. Naturforsch* **1980**, *35a* (1), 98–102.

(17) White, N. A. S.; Ellis, H. A. *J. Mol. Struct.* **2008**, *888* (1−3), 386–393.
(18) White, N. A. S.; Ellis, H. A. *Mol. Cryst. Liq. Cryst.* **2009**, *501*, 28–42.
(19) Gallot, B.; Skoulios, A. *Kolloid Z. Z. Polym.* **1966**, *209* (2), 164–169.
(20) Vold, M. J.; Funakoshi, H.; Vold, R. D. *J. Phys. Chem.* **1976**, *80* (16), 1753–1761.
(21) Busico, V.; Ferraro, A.; Vacatello, M. *J. Phys. Chem.* **1984**, *88* (18), 4055–4058.
(22) Skoda, W. *Kolloid Z. Z. Polym.* **1969**, *234* (2), 1128–1138.
(23) Enders-Beumer, A.; Harkema, S. *Acta Crystallogr. B* **1973**, *29*, 682–685.
(24) Amirthalingam, V.; Padmanabhan, V. M. *Acta Crystallogr.* **1958**, *11*, 896.
(25) Galigne, J. L.; Mouvet, M.; Falgueirettes, J. *Acta Crystallogr. B* **1970**, *26*, 368.
(26) Martínez Casado, F. J.; Ramos Riesco, M.; Sánchez Arenas, A.; García Pérez, M. V.; Redondo, M. I.; López-Andrés, S.; Garrido, L.; Cheda, J. A. R. *J. Phys. Chem. B* **2008**, *112* (51), 16601–16609.
(27) Barman, S.; Venkataraman, N. V.; Vasudevan, S.; Seshadri, R. *J. Phys. Chem. B* **2003**, *107*, 1875–1883.
(28) Asayama, R.; Kawamura, J.; Hattori, T. *Chem Phys. Lett.* **2005**, *414* (1−3), 87–91.
(29) (a) Mc Bain, J. W.; Stewart, A. *J. Phys. Chem.* **1933**, *37*, 675–684. (b) Mc Bain, J. W.; Field, M. C. *J. Phys. Chem.* **1933**, *37*, 920–924.
(30) Fernández-García, M.; Cheda, J. A. R.; Westrum, E. F.; Fernández-Martín, F. J. *Colloid Interface Sci.* **1997**, *185*, 371–381.
(31) Fernández-García, M.; García, M. V.; Redondo, M. I.; Cheda, J. A. R.; Fernández-García, M.; Westrum, E. F.; Fernández-Martín, F. *J. Lipid Res.* **1997**, *38*, 361–372.
(32) Brouwer, H. W.; Spier, H. L. *Proc. 3rd Int. Conf. Therm. Anal.* **1971**, *3*, 131–144.
(33) Meisel, T.; Seybold, K.; Halmos, Z.; Roth, J.; Melykuty Cs, *J. Therm. Anal.* **1976**, *10*, 419–431.
(34) Kung, H. C.; Goddard, E. D. *J. Colloid Interface Sci.* **1969**, *39*, 242–249.
(35) Goddard, E. D.; Goldwasser, S.; Golikeri, G.; Kung, H. C. *Adv. Chem. Ser.* **1968**, *84*, 67–77.
(36) Sheldrick, G. M. *SHELXS 97*; University of Göttingen: Germany 1997.
(37) Sheldrick, G. M. *SHELXL 97*; University of Göttingen: Germany 1997.
(38) Lomer, T. R. *Acta Crystallogr.* **1952**, *5*, 11–14.
(39) Bird, M. J.; Lomer, T. R. *Acta Crystallogr. B* **1972**, *28*, 242–246.
(40) Lacouture, F.; Francois, M.; Didierjean, C.; Rivera, J. P.; Rocca, E.; Steinmetza, J. *Acta Crystallogr. C* **2001**, *57*, 530–531.
(41) Taylor, R. A.; Ellis, H. A. *Acta Crystallogr.* **2008**, *E64*, m895.
(42) Skoda, W. *Kolloid Z. Z. Polym.* **1969**, *234* (2), 1128–1138.
(43) Gallot, B.; Skoulios, A. *Kolloid Z. Z. Polym.* **1966**, *210* (2), 143–149.
(44) Olsher, U.; Izatt, R. M.; Bradshaw, J. S.; Dalley, N. K. *Chem. Rev.* **1991**, *91* (2), 137–164.
(45) Kitagawa, S.; Kitaura, R.; Noro, S. *Angew. Chem., Int. Ed.* **2004**, *42*, 2334–2375.
(46) Mirnaya, T. A.; Yaremchuk, G. G.; Prisyazhnyi, V. D. *Liq. Cryst.* **1990**, *8*, 701–705.
(47) Sato, K.; Kobayashi, W. *Crystals, Growth, Properties and Applications: Organic crystals*; Kare, N., Ed.; Springer-Verlag: Berlin, 1991; Vol. 1, pp 65−108.
(48) Cingolani, A.; Spinolo, G.; Sanesi, M. *Z. Naturforsch.* **1979**, *34a* (5), 575–578.
(49) George, A. M.; Richet, P.; Stebbins, J. F. *Am. Mineral.* **1998**, *83*, 1277–1284.
(50) Ubbelohde, A. R. *The Molten State of Matter: Melting and Cristal Structure*; Wiley J.:New York, 1978.
(51) Franzosini, P.; Sanesi, M. *Thermodynamic and transport properties of organic salts*; Pergamon Press: Oxford, 1980.
(52) Hainovsky, N.; Maier, J. *Phys. Rev. B* **1995**, *51* (22), 15789–15797.
(53) Arnold, T.; Cook, R. E.; Chanaa, S.; Clarke, S. M.; Farinelli, M.; Yaron, P.; Larese, J. Z. *Physica B* **2006**, *385−386* (1), 205–207.
(54) Takeda, S.; Fujiwara, T.; Chihara, H. *J. Phys. Soc. Jpn.* **1989**, *58*, 1793–1800.
(55) Nicolai, B.; Cousson, A.; Fillaux, F. *Chem. Phys.* **2003**, *290*, 101–120.
(56) Bolhuis, P.; Hagen, M.; Frenkel, D. *Phys. Rev. E* **1994**, *50* (6), 4880–4890.
(57) Tejero, C. F.; Daanoun, A.; Lakkerkerker, H. N. W.; Baus, M. *Phys. Rev. E* **1995**, *51* (1), 558–566.
(58) Dijkstra, M.; Van Roij, R.; Evans, R. *Phys. Rev. Lett.* **1998**, *81* (11), 2268–2271.
(59) Herbstein, F. H. *Acta Cryst. B* **2006**, *62*, 341–383.
(60) Gafner, G.; Herbstein, F. H. *Acta Cryst.* **1960**, *13*, 706−716; **1964**, *17*, 982−985.
(61) Bendeif, E. E.; Dahaoui, S.; François, M.; Benali-Cherif, N.; Lecomte, C. *Acta Cryst. B* **2005**, *61*, 700–709.
(62) Strobl, G.; Ewen, B.; Fischer, E. W.; Piesczek, W. *J. Chem. Phys.* **1974**, *61* (12), 5257–5264.
(63) Busico, V.; Ferraro, A.; Vacatello, M. *J. Phys. Chem.* **1984**, *88* (18), 4055–4058.
(64) Sirota, E. B. *Langmuir* **1997**, *13* (14), 3849–3859.
(65) Vollhardt, D. *J. Phys. Chem. C* **2007**, *111* (8), 6805–6812.
(66) Spitalsky, Z.; Bleha, T. *Macromol. Theory Simul.* **2001**, *10* (9), 833–841.

JP9047715